

# Time-dependent coupled-cluster method for atomic nuclei

D. A. Pigg,<sup>1,2</sup> G. Hagen,<sup>2,3</sup> H. Nam,<sup>4</sup> and T. Papenbrock<sup>3,2</sup>

<sup>1</sup>*Department of Physics and Astronomy, Vanderbilt University, Nashville, Tennessee 37235, USA*

<sup>2</sup>*Physics Division, Oak Ridge National Laboratory, Oak Ridge, Tennessee 37831, USA*

<sup>3</sup>*Department of Physics and Astronomy, University of Tennessee, Knoxville, Tennessee 37996, USA*

<sup>4</sup>*National Center for Computational Sciences Division,  
Oak Ridge Leadership Computing Facility, Oak Ridge National Laboratory,  
P.O. Box 2008, Oak Ridge, Tennessee 37831, USA*

(Dated: March 4, 2013)

We study time-dependent coupled-cluster theory in the framework of nuclear physics. Based on Kvaal's bi-variational formulation of this method [S. Kvaal, arXiv:1201.5548], we explicitly demonstrate that observables that commute with the Hamiltonian are conserved under time evolution. We explore the role of the energy and of the similarity-transformed Hamiltonian under real and imaginary time evolution and relate the latter to similarity renormalization group transformations. Proof-of-principle computations of  ${}^4\text{He}$  and  ${}^{16}\text{O}$  in small model spaces, and computations of the Lipkin model illustrate the capabilities of the method.

PACS numbers: 21.60.-n, 24.50.+g, 31.15.bw

## I. INTRODUCTION

Coupled-cluster (CC) theory was introduced in nuclear physics by Coester and Kümmel [1, 2] more than 50 years ago, and Cizek and Paldus [3–5] further developed the method for applications in quantum chemistry. For reviews of this method we refer the reader to Refs. [6–9]. The popularity of coupled-cluster theory is due to the attractive compromise the method offers between accuracy on the one hand and computational cost on the other hand. In nuclear structure and reactions, for instance, the method has extended the reach of *ab initio* computations from light  $p$  shell nuclei [10] to medium-mass nuclei [11, 12].

Time-dependent coupled-cluster (TDCC) theory dates back more than 30 years. It was proposed by Hoodbhoy and Negele [13, 14], with the aim to describe nuclear collisions, and by Schönhammer and Gunnarson [15] to compute spectral functions. Until now, however, nuclear collision processes are usually described within time-dependent mean-field methods [16–20]. Likewise, applications of TDCC in quantum chemistry have only been sporadic [21–28]. For small amplitude oscillations, time-dependent coupled-cluster theory leads to the computation of excited states within linear response theory, and the method is routinely used [21, 25, 29] in this framework. However, the situation is different for large-amplitude oscillations. We believe that this lack of popularity is mainly due to conceptual problems regarding the conservation of energy, and keeping the energy a real (and not complex) number [28]. These aspects have only been clarified very recently in Kvaal's formulation [30] of TDCC as a bi-variational theory [31], and the result is a real energy that is conserved under time evolution. This approach opens the way to many exciting applications. In this work, we present a formal proof regarding the conservation of energy within Kvaal's formulation of TDCC and also show that observables that

commute with the Hamiltonian are conserved under time evolution. We study in detail the role of the similarity-transformed Hamiltonian under real and imaginary time evolution and illustrate our results in applications to the nuclei  ${}^4\text{He}$  and  ${}^{16}\text{O}$  in small model spaces and to the Lipkin model.

This paper is organized as follows. In Sect. II, we re-derive TDCC, set it in relation to time-independent CC, and discuss formal aspects about conserved quantities. In Sect. III we focus on the energy. We explicitly demonstrate that the numerical time-evolution of the bi-variational CC theory preserves the energy. We also study the real and imaginary time-evolution of the similarity-transformed Hamiltonian. In Sect. IV we discuss applications of the method. First, we show that the Fourier analysis of the time-evolved coupled-cluster amplitudes of the nuclei  ${}^4\text{He}$  and  ${}^{16}\text{O}$  yields excitation spectra. Second, we study the Lipkin model and compare our results for observables with exact results. We finish with our conclusions. Technical aspects are relegated to the Appendix.

## II. COUPLED-CLUSTER THEORY

In this Section, we briefly re-derive the equations that govern TDCC theory and prove that observables that commute with the Hamiltonian are conserved under time evolution. We also consider TDCC in the limit of linear response theory, and the limit of vanishing time dependence.

### A. Time-dependent coupled-cluster equations

We are interested in solving the time-dependent Schrödinger equation

$$H(t) |\Psi(t)\rangle = i\hbar \partial_t |\Psi(t)\rangle. \quad (1)$$

Here  $H(t)$  is a time-dependent Hamiltonian. In TDCC theory, the many-body wave function results from an exponential excitation operator acting on a product state

$$|\Psi\rangle = e^{S(t)} |\Phi\rangle. \quad (2)$$

Here

$$|\Phi\rangle = \prod_{p=1}^A a_p^\dagger(t) |0\rangle \quad (3)$$

is an  $A$ -body product state that serves as the reference state. The creation operator  $a_p^\dagger$  creates a fermion in the single-particle state  $p$ , while an annihilation operator  $a_p$  would remove a fermion from the single-particle state  $p$ . The creation and annihilation operators are allowed to depend on time, and they fulfill the usual anti-commutation relations at equal times. The time dependence of the creation and annihilation operators is [14]

$$\partial_t a_q^\dagger(t) = \sum_p \langle p(t) | \dot{q}(t) \rangle a_p^\dagger(t). \quad (4)$$

Here  $|q(t)\rangle = a_q^\dagger(t) |0\rangle$  and  $|\dot{q}(t)\rangle$  denotes the time derivative of  $|q(t)\rangle$ . To simplify notation, we will suppress the explicit time argument and denote  $a_q(t)$  as  $a_q$  and  $|q(t)\rangle$  as  $|q\rangle$ . In Eq. (2) the cluster operator  $S(t)$  is

$$S(t) = s_0(t) + S_1(t) + S_2(t) + S_3(t) + \dots + S_A(t). \quad (5)$$

Here  $s_0(t)$  is a complex phase while the operators  $S_1(t), \dots, S_A(t)$  generate  $1p-1h$ ,  $2p-2h$ ,  $3p-3h$ , and up to  $Ap-Ah$  excitations within the reference state  $|\Phi\rangle$ , with

$$S_n(t) = \frac{1}{(n!)^2} \sum_{i_1 \dots i_n, a_1 \dots a_n} s_{i_1 \dots i_n}^{a_1 \dots a_n}(t) a_{a_1}^\dagger \dots a_{a_n}^\dagger a_{i_n} \dots a_{i_1}. \quad (6)$$

The functions  $s_0(t)$  and  $s_{i_1 \dots i_n}^{a_1 \dots a_n}(t)$  are the unknown time-dependent excitation amplitudes. In what follows, we also suppress the explicit time argument of the  $np-nh$  cluster operators  $S_n(t)$ , the phase  $s_0(t)$ , and the excitation amplitudes  $s_{i_1 \dots i_n}^{a_1 \dots a_n}(t)$ . In addition, we will use the indices  $i, j, k, \dots$  and  $a, b, c, \dots$  to label occupied and unoccupied states in the reference (3), respectively, and the indices  $p, q, r, \dots$  to label any state.

We are interested in the time evolution of the cluster operator  $S$ . For computational efficiency, we employ the coupled-cluster with singles-and-doubles (CCSD) approximation and truncate  $S$  at the  $2p-2h$  excitation level

$$\begin{aligned} S &= s_0 + S_1 + S_2 \\ &= s_0 + \sum_{ia} s_i^a a_a^\dagger a_i + \frac{1}{4} \sum_{ijab} s_{ij}^{ab} a_a^\dagger a_b^\dagger a_j a_i. \end{aligned} \quad (7)$$

To derive the equations of motion for the amplitudes  $s_0$ ,  $s_i^a$ , and  $s_{ij}^{ab}$  we left-multiply the time-dependent Schrödinger equation (1) with the operator  $e^{-S}$ , such that

$$\overline{H} |\Phi\rangle = i\hbar e^{-S} \partial_t e^S |\Phi\rangle. \quad (8)$$

Here, we introduced the similarity-transformed Hamiltonian

$$\overline{H} \equiv e^{-S} H e^S \quad (9)$$

For the computation of the similarity transformation  $\overline{B} \equiv e^{-S} B e^S$  of an operator  $B$  we use the Baker-Campbell-Hausdorff expansion,

$$\begin{aligned} e^{-S} B e^S &= B + [B, S] + \frac{1}{2!} [[B, S], S] \\ &+ \frac{1}{3!} [[[B, S], S], S] \\ &+ \frac{1}{4!} [[[[B, S], S], S], S] + \dots \end{aligned} \quad (10)$$

For a two-body operator, this expansion truncates naturally at its fourth nested commutator. For  $B = \partial_t$ , the expansion in Eq.(10) reduces to

$$e^{-S} \partial_t e^S = \partial_t + \dot{S} + \frac{1}{2} [\dot{S}, S] \quad (11)$$

for any truncation of  $S$ . Note that the commutator  $[\dot{S}, S]$  is only nonzero if the single-particle states depend explicitly on time [see Eq. (4)].

We insert the CCSD ansatz (7) into Eq. (8); left-project with the Hermitian adjoints of the states  $|\Phi\rangle$ ,  $|\Phi_i^a\rangle \equiv a_a^\dagger a_i |\Phi\rangle$ , and  $|\Phi_{ij}^{ab}\rangle \equiv a_a^\dagger a_b^\dagger a_j a_i |\Phi\rangle$ ; and then use Eq. (11). In what follows, we limit ourselves to time-independent basis functions. The equations of motion for the  $S$  amplitudes within a time-dependent basis are presented in Appendix A. We obtain

$$i\hbar \dot{s}_0 = \langle \Phi | \overline{H} | \Phi \rangle, \quad (12)$$

$$i\hbar \dot{s}_i^a = \langle \Phi_i^a | \overline{H} | \Phi \rangle, \quad (13)$$

$$i\hbar \dot{s}_{ij}^{ab} = \langle \Phi_{ij}^{ab} | \overline{H} | \Phi \rangle. \quad (14)$$

The left-hand sides of these equations are matrix elements of the similarity-transformed Hamiltonian  $\overline{H} \equiv e^{-S} H e^S$ . The corresponding algebraic expressions can be worked out diagrammatically and are well known from time-independent CCSD [7, 9]. The resulting expressions are linear in the matrix elements of the Hamiltonian and nonlinear in the cluster amplitudes. It is useful to rewrite the equations (12) to (14) in operator form as

$$i\hbar \dot{S} = \overline{H}_1. \quad (15)$$

Here  $\overline{H}_1$  denotes the operator that is obtained from the similarity-transformed Hamiltonian  $\overline{H}$  when all but the matrix elements on the right hand side of Eqs. (12-14) are set to zero. When viewing  $\overline{H}$  as a matrix (See Eq. (45))

below), the first column of the matrix of  $\bar{H}_1$  is thus identical to the first column of  $\bar{H}$ , while all other columns are zero.

For the computation of observables within TDCC we follow Ref. [30]. Coupled-cluster theory employs a non-Hermitian Hamiltonian  $\bar{H}$  and must thus be formulated in a bi-variational approach, i.e. the left (bra) and right (ket) states must be varied independently. In this formulation, the energy expectation value is

$$E = \langle \Phi | L \bar{H} | \Phi \rangle. \quad (16)$$

Here  $L$  is a linear de-excitation operator

$$L = l_0 + \sum_{ia} l_a^i a_i^\dagger a_a + \frac{1}{4} \sum_{ijab} l_{ab}^{ij} a_i^\dagger a_j^\dagger a_b a_a, \quad (17)$$

and  $l_0$ ,  $l_a^i$ , and  $l_{ab}^{ij}$  are the amplitudes associated with up to  $2h$ - $2p$  de-excitations [9]. From Eq. (16), it is clear that the left many-body state is given by

$$\langle \Psi_L | \equiv \langle \Phi | L e^{-S}. \quad (18)$$

To obtain the time evolution of the operator  $L$ , we insert  $\langle \Psi_L |$  of Eq. (18) into the time-dependent Schrödinger equation, right-multiply by  $e^S$  and obtain

$$-i\hbar \dot{L}_0 = 0, \quad (19)$$

$$-i\hbar \dot{l}_a^i = \langle \Phi | L \bar{H} | \Phi_i^a \rangle, \quad (20)$$

$$-i\hbar \dot{l}_{ab}^{ij} = \langle \Phi | L \bar{H} | \Phi_{ij}^{ab} \rangle. \quad (21)$$

Again, we can write these equations in operator form as

$$-i\hbar \dot{L} = L \bar{H} - L \bar{H}_1, \quad (22)$$

and here it is understood that the right hand side, when written in matrix form of Eq. (45), has nonzero matrix elements in all but the first row. Note that  $l_0 = 1$  for proper normalization.

Let us explicitly check that the energy (16) is conserved. From the definition  $\bar{H} = e^{-S} H e^S$  and Eq. (15) we find

$$\dot{\bar{H}} = [\bar{H}, \dot{S}] = -\frac{i}{\hbar} [\bar{H}, \bar{H}_1]. \quad (23)$$

Thus

$$\begin{aligned} \dot{E} &= \langle \Phi | \dot{L} \bar{H} | \Phi \rangle + \langle \Phi | L \dot{\bar{H}} | \Phi \rangle \\ &= \frac{i}{\hbar} \left( \langle \Phi | (L \bar{H} - L \bar{H}_1) \bar{H} | \Phi \rangle \right. \\ &\quad \left. + \langle \Phi | L \bar{H}_1 \bar{H} | \Phi \rangle - \langle \Phi | L \bar{H} \bar{H}_1 | \Phi \rangle \right) \\ &= 0. \end{aligned} \quad (24)$$

Here we used Eq. (22) and  $\bar{H} | \Phi \rangle = \bar{H}_1 | \Phi \rangle$ .

We can extend these results to any observable  $B$  that commutes with the Hamiltonian. We have for the expectation value  $\langle B \rangle \equiv \langle \Phi | L \bar{B} | \Phi \rangle$

$$\begin{aligned} \langle \dot{B} \rangle &= \langle \Phi | \dot{L} \bar{B} | \Phi \rangle + \langle \Phi | L \dot{\bar{B}} | \Phi \rangle \\ &= \frac{i}{\hbar} \langle \Phi | L [\bar{H}, \bar{B}] | \Phi \rangle \\ &= 0. \end{aligned} \quad (25)$$

Here, we used  $\dot{\bar{B}} = (i/\hbar) [\bar{H}, \bar{B}]$  as the generalization of Eq. (23), and  $[\bar{H}, \bar{B}] = 0$  follows from  $[H, B] = 0$ . Note that this proof addresses a long-standing problem already raised by Monkhorst [24].

For the computation of observables, one employs the normal-ordered one-body and two-body density matrices

$$(\rho_{qp}^n)_N = \langle \Phi | L e^{-S} \{p^\dagger q\} e^S | \Phi \rangle_C, \quad (26)$$

$$(\rho_{rspq}^n)_N = \langle \Phi | L e^{-S} \{p^\dagger q^\dagger sr\} e^S | \Phi \rangle_C. \quad (27)$$

Here, only connected ( $C$ ) diagrams contribute. Due to the linearity of  $L$ , these densities have finite expansions.

## B. Time-independent coupled-cluster equations

Let us re-derive the well-known time-independent CCSD equations from TDCC theory by requiring that the cluster operators  $S_1$  and  $S_2$ , and the single-particle basis do not depend on time. Thus we obtain from the Eqs. (13) and (14)

$$\langle \Phi_i^a | \bar{H} | \Phi \rangle = 0, \quad (28)$$

$$\langle \Phi_{ij}^{ab} | \bar{H} | \Phi \rangle = 0. \quad (29)$$

These are the time-independent CCSD equations. They state that the reference state  $|\Phi\rangle$  is an eigenstate of the similarity-transformed Hamiltonian  $\bar{H}$  in the space of  $1p$ - $1h$  and  $2p$ - $2h$  excitations. Thus the corresponding eigenvalue is the energy

$$E_0 = \langle \Phi | \bar{H} | \Phi \rangle, \quad (30)$$

and Eq. (12) yields

$$s_0 = -\frac{i}{\hbar} E t \quad (31)$$

up to an irrelevant constant.

## C. Coupled-cluster equations of motion

The equation-of-motion CC methods [25, 32] are commonly used to compute excited states within the CC method. For completeness, we briefly re-derive the corresponding equations from the time-dependent formalism. Again, we assume that the Hamiltonian and the single-particle basis do not explicitly depend on time. For the solutions of Eqs. (13) and (14), we make the ansatz

$$\begin{aligned} s_i^a(t) &= t_i^a + r_i^a(t), \\ s_{ij}^{ab}(t) &= t_{ij}^{ab} + r_{ij}^{ab}(t), \end{aligned} \quad (32)$$

assume that the time-independent amplitudes  $t_i^a$  and  $t_{ij}^{ab}$  fulfill the time-independent CCSD equations (28,29), and that the remainders  $r_i^a$  and  $r_{ij}^{ab}$  are small perturbations, i.e.  $S = T + R$  with  $|R| \ll |T|$ . In leading order we thus have

$$\bar{H} \approx e^{-T} H e^T \equiv \bar{H}_T. \quad (33)$$

We insert  $S = T + R$  into Eq. (15), employ Eqs. (28), (29), and the expansion (10), and keep only the terms first-order in  $R$ . This yields the operator equation

$$i\hbar\dot{R} = \bar{H}_T + [\bar{H}_T, R]. \quad (34)$$

Then, assuming, a simple harmonic time-dependence,

$$r_i^a(t) = r_i^a e^{-i\omega t} \quad (35)$$

$$r_{ij}^{ab}(t) = r_{ij}^{ab} e^{-i\omega t}, \quad (36)$$

we find that the amplitudes and frequencies solve the eigenvalue problem

$$\begin{aligned} \hbar\omega r_i^a &= \langle \Phi_i^a | [\bar{H}_T, R] | \Phi \rangle, \\ \hbar\omega r_{ij}^{ab} &= \langle \Phi_{ij}^{ab} | [\bar{H}_T, R] | \Phi \rangle. \end{aligned} \quad (37)$$

These are the well known equations of motion for the computation of excited states within CCSD.

It is also interesting to study the left equation (22) for  $S = T + R$ , with  $|R|, |L| \ll T$ . Keeping terms linear in  $R$  and  $L$  yields in leading order

$$-i\hbar\dot{L} = L(\bar{H}_T - E_0) \quad (38)$$

since  $(\bar{H}_T)_1 = E_0$ . Again we assume a harmonic time-dependence

$$l_a^i(t) = l_a^i e^{i\omega t}, \quad (39)$$

$$l_{ab}^{ij}(t) = l_{ab}^{ij} e^{i\omega t}, \quad (40)$$

and find the well-known left eigenvalue problem

$$L\bar{H}_T = (E_0 + \omega)L. \quad (41)$$

### III. ROLE OF ENERGY

In this Section, we focus on the role of the energy in TDCC theory. First, we probe the conservation of energy (24) numerically for simple models of light nuclei. Next, we study the time-dependent eigenvalues of the similarity-transformed Hamiltonian  $\bar{H}$  and find that these cannot be viewed as energies. This opens the way to employ imaginary-time evolutions of the similarity-transformed Hamiltonian for the computation of the ground-state energy. In what follows we employ a low-momentum two-body interaction produced by a similarity renormalization group transformation [33] of the  $N^3\text{LO}$  interaction from chiral effective field theory [34] at the cutoff  $\Lambda = 1.9 \text{ fm}^{-1}$ . We use a small model space of four oscillator shells. For the time integration of  $S$  and  $L$  according to Eqs. (15) and (22), we employ the fourth-order Runge-Kutta method.

#### A. Time evolution of the energy functional

For the time evolution, we iteratively solve Eqs. (15) and (22). We set  $l_0 = 1$  and neglect the complex phase

$s_0$ , and periodically compute the difference between the total energy, according to Eq. (16), and its initial value. Figure 1 shows this difference in total binding energy as a function of time for the  ${}^4\text{He}$  nucleus with a time step of width 0.05 fm/c. The change in energy is very small throughout the time-evolution and energy is conserved for all practical purposes. In practice, the precision to which the method conserves energy has a notable dependence on the time step width: we obtain changes to energy on the order of  $10^{-10}$  MeV using a step width of 0.05 fm/c and changes to energy of average order  $10^{-2}$  MeV for a step width of 1 fm/c.

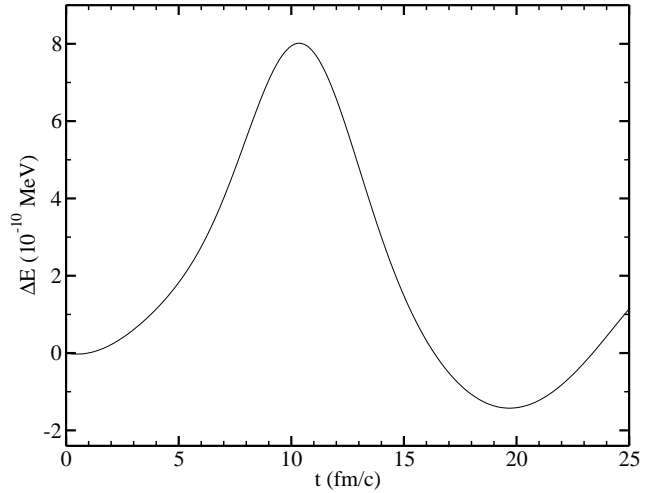


FIG. 1: The time evolution of the change in total energy of  ${}^4\text{He}$  from its initial value.

#### B. Time evolution of $\bar{H}$

We are interested in the eigenvalues of the similarity-transformed Hamiltonian (9). For a time-independent Hamiltonian  $H$ , the eigenvalues of  $\bar{H}$  do not depend on time if the similarity transformation is carried out exactly. For an  $A$ -body system, a complete model space consists of up to  $Ap$ - $Ah$  excitations of the reference state, but this is computationally not feasible in general. Instead, one chooses a model space of up to  $2p$ - $2h$  excitations within the CCSD approximation. This truncation renders the similarity transformation inexact and it is thus no surprise that the eigenvalues of  $\bar{H}$  are not constant in time.

To illustrate the effects of the truncations, we consider three distinct cases. (i) In the case “TD-CCSD ( $2p$ - $2h$ ),” we employ  $S = S_1 + S_2$  in the computation of  $\bar{H}$  [i.e. we time evolve the  $S$  amplitudes according to Eqs. (13) and (14)], and compute the lowest eigenvalue of  $\bar{H}$  within a basis including up to  $2p$ - $2h$  excited states. Clearly, this case has truncations in the model space for nuclei with  $A > 2$ . (ii) In the case “TD-CCS

(2p-2h),” we employ  $S = S_1$  [i.e. we set  $S_2 = 0$ , solve the time-dependent coupled-cluster singles (CCS) equation (13)]. We compute the ground-state energy within a basis including up to 2p-2h excited states. Here, the similarity-transformation is simpler than in case (i), but the model space is incomplete for nuclei with  $A > 2$ . (iii) In the case “TD-CCS (3p-3h),” we again solve the time-dependent CCS equation (13), but compute the ground-state energy within a basis including up to 3p-3h excited states  $|\Phi_{ijk}^{abc}\rangle$ . Here, no approximation is made for a nucleus with  $A = 3$ . In what follows we will consider these distinct cases for nuclei with mass number  $A = 3$  and  $A = 4$ .

Figure 2 shows the eigenvalues of the similarity-transformed Hamiltonian of  $^3\text{H}$  as a function of time for the three cases discussed above. As expected, the energy is only conserved for case (iii). Case (i) and (ii) are different similarity transformations and yield different  $\bar{H}$ .

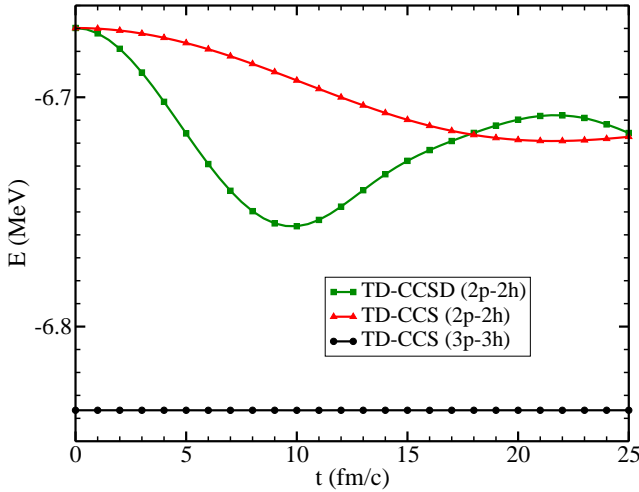


FIG. 2: (Color online) The time evolution of the lowest eigenvalue of the similarity-transformed Hamiltonian  $\bar{H}$  for  $^3\text{H}$  computed for three distinct cases (see text for details).

Figure 3 shows the eigenvalues of the similarity-transformed Hamiltonian of  $^4\text{He}$  as a function of time for the three cases discussed above. As expected, the energy is not conserved in any of the cases. The fluctuations of the energy are smallest for case (iii) which exhibits the least truncation.

The results of this subsection explain clearly why matrix elements [28] or eigenvalues of the similarity-transformed Hamiltonian cannot serve as conserved energies. However, these results also open up the possibility to employ imaginary-time evolution as a projection technique.

### C. Imaginary-time evolution of $\bar{H}$

Imaginary time propagation of a given quantum state projects out the lowest-energy state that has a nonzero

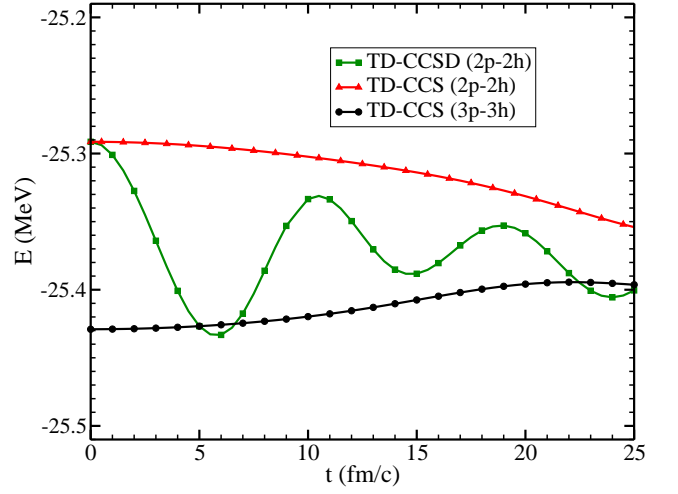


FIG. 3: (Color online) Same as Fig. 2 but for  $^4\text{He}$

overlap with this state. We set  $t = -i\hbar\tau$  with real  $\tau$  and obtain the evolution equations

$$\partial_\tau s_i^a = -\langle \Phi_i^a | e^{-S} H e^S | \Phi \rangle, \quad (42)$$

$$\partial_\tau s_{ij}^{ab} = -\langle \Phi_{ij}^{ab} | e^{-S} H e^S | \Phi \rangle \quad (43)$$

from Eqs. (13) and (14). It is useful to consider the imaginary time evolution of the Hamiltonian directly. The corresponding evolution equation is

$$\partial_\tau \bar{H}(\tau) = [\bar{H}(\tau), \partial_\tau S]. \quad (44)$$

Eq. (44) shows that  $\partial_\tau S$  generates the similarity transformation of the Hamiltonian. It is similar to the similarity renormalization group equations employed in taming interactions [35–37] and in computations of finite nuclei [38]. The evolution stops (i.e. it reaches a fixed point) once the right hand side of Eq. (44) vanishes. At the fixed point the matrix elements of  $\bar{H}$  fulfill the time-independent CCSD Eqs. (28,29). Thus, the imaginary time evolution emerges as an alternative way of solving the coupled-cluster equations.

As an example, we consider the imaginary time evolution for  $^4\text{He}$ . For the initial conditions we choose  $s_i^a = 0 = s_{ij}^{ab}$ . We then propagate  $s_i^a$  and  $s_{ij}^{ab}$  according to Eqs. (42) and (43) while periodically computing the ground-state energy as the right eigenvalue of  $\bar{H}$ . Figure 4 shows the difference  $\Delta E = |E(\tau) - E_{\text{CCSD}}|$  as a function of  $\tau$ , obtained using 400 steps of width 0.5 fm/c. Here,  $E_{\text{CCSD}}$  is the energy that one can obtain from solving the CCSD equations (28,29) directly. The convergence to the ground state energy is exponentially fast, and the exponent is related to the energy gap to the first excited state.

Let us also visualize the evolution of the  $\tau$ -dependent similarity-transformed Hamiltonian. We present the

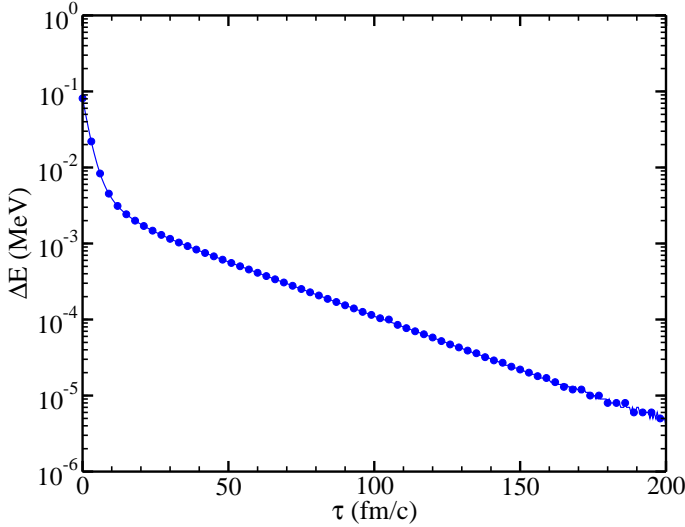


FIG. 4: (Color online) The magnitude of the difference between the total energy and CCSD ground-state energy for  ${}^4\text{He}$  as a function of imaginary time  $\tau$ .

Hamiltonian in a block format as

$$\bar{H} = \begin{pmatrix} \langle \Phi | \bar{H} | \Phi \rangle & \langle \Phi | \bar{H} | \Phi_k^c \rangle & \langle \Phi | \bar{H} | \Phi_{kl}^{cd} \rangle \\ \langle \Phi_i^a | \bar{H} | \Phi \rangle & \langle \Phi_i^a | \bar{H} | \Phi_k^c \rangle & \langle \Phi_i^a | \bar{H} | \Phi_{kl}^{cd} \rangle \\ \langle \Phi_{ij}^{ab} | \bar{H} | \Phi \rangle & \langle \Phi_{ij}^{ab} | \bar{H} | \Phi_k^c \rangle & \langle \Phi_{ij}^{ab} | \bar{H} | \Phi_{kl}^{cd} \rangle \end{pmatrix} \quad (45)$$

and plot logarithms of the averages of the magnitudes of all elements within a given block. Figure 5 shows contour plots of these averages taken at  $\tau = 0$  fm/c and  $\tau = 200$  fm/c, with a step size of  $\delta\tau = 0.5$  fm/c. We see that the Hamiltonian is driven to a form that makes the reference state  $|\Phi\rangle$  a right eigenstate and the element  $\langle \Phi | \bar{H} | \Phi \rangle$  the corresponding eigenvalue. At  $\tau = 200$  fm/c the time-independent CCSD Eqs. (28) and (29) have practically been solved.

#### IV. APPLICATIONS

In this Section we study two applications of the TDCC method. First, we compute the spectra of excited state energies for  ${}^4\text{He}$  and  ${}^{16}\text{O}$  as the Fourier transforms of the time-evolved cluster amplitudes and compare the results to those obtained by solving the time-independent coupled-cluster equations of motion. Second, we revisit the interacting Lipkin system and compare with the results by Hoodbhoy and Negele [13].

##### A. Energy spectra from Fourier transforms

In coupled-cluster theory, the standard approach to excited states [25, 32] is the solution of the right eigen-

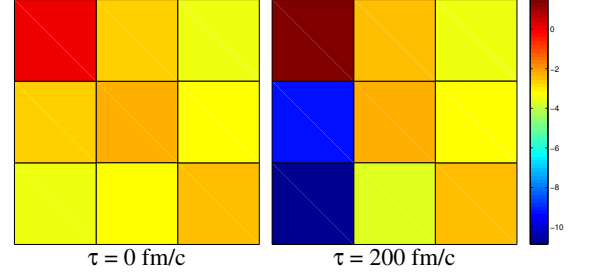


FIG. 5: (Color online) Logarithmic averages over the elements of  $\bar{H}(\tau)$  for  ${}^4\text{He}$  at  $\tau = 0$  fm/c and  $\tau = 200$  fm/c, where  $\bar{H}(\tau)$  has the form given in (45).

value problem (37). Alternatively, we can obtain a spectrum of excited-state energies from a Fourier transformation of any of the time-evolved CCSD amplitudes  $s_i^a$  and  $s_{ij}^{ab}$ , utilizing the solution of Eq. (15). This approach involves first solving the time-independent CCSD equations, Eqs. (28) and (29). Then, we perturb the resulting cluster amplitudes by a small random contribution of the order  $\approx 0.001$  and solve Eqs. (13) and (14). During the iterations, we record the time evolution of a single, randomly-selected amplitude  $s_i^a$  or  $s_{ij}^{ab}$ . Results for the Fourier transform of the CCSD amplitudes for  ${}^4\text{He}$  and  ${}^{16}\text{O}$  are shown in Fig. 6 and Fig. 7, respectively. The length of the time evolution is 20000 fm/c for  ${}^4\text{He}$  and 6000 fm/c for  ${}^{16}\text{O}$ , and the step size is 1 fm/c. Corresponding to the length of the time evolution, the energy uncertainty in the resulting Fourier spectra is about  $\delta E \approx 0.06$  MeV for  ${}^4\text{He}$  and  $\delta E \approx 0.2$  MeV for  ${}^{16}\text{O}$ . In each plot (the excitation energies are measured relative to the ground state) the giant peaks at  $E = 0$  correspond to the ground-state of each system. Note that several of the excited-state energies shown in Figs. 6 and 7 are not associated with physical states of  ${}^4\text{He}$  or  ${}^{16}\text{O}$ , respectively but arise from the limitation of a small model space, and the incomplete separation of the center-of-mass motion [39]. In Tables I and II, for  ${}^4\text{He}$  and  ${}^{16}\text{O}$ , respectively, we compare the values associated with four selected peaks to the values computed using equation-of-motion CCSD. Note that all of the peaks in Figs. 6 and 7 are associated with energies computed with this method. The agreement is good, and deviations are within the uncertainties related to the finite time evolution.

Note that TDCC calculation of excited states via Fourier transformation requires much more computational cycles than the standard approach. The latter requires us to solve the eigenvalue problem (37) once,

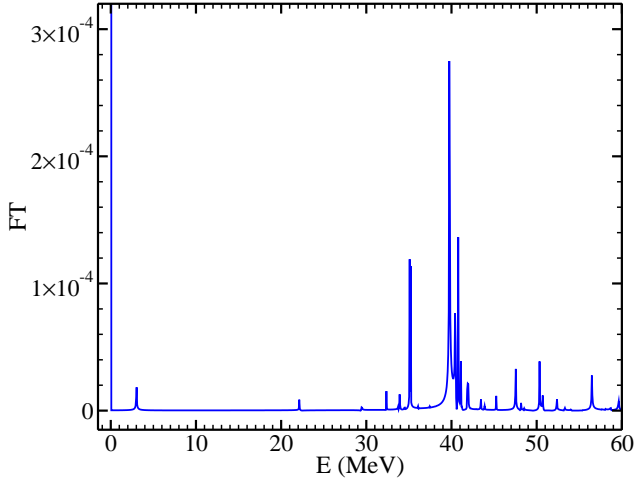


FIG. 6: (Color online) Fourier transform of a randomly-selected cluster amplitude  $s_i^a$  or  $s_{ij}^{ab}$  for  ${}^4\text{He}$ . Energies are measured relative to the ground-state energy.

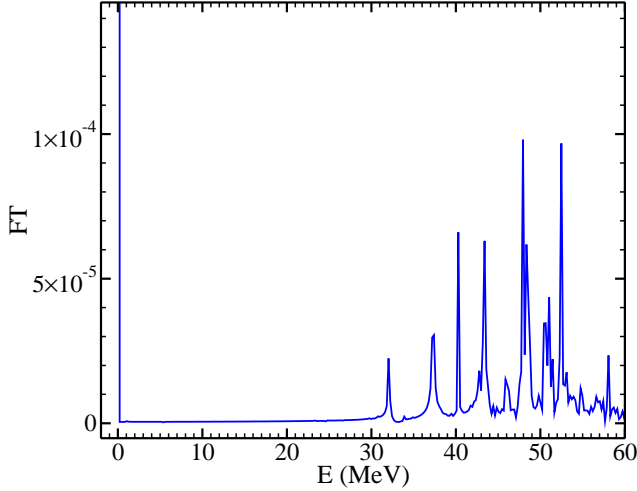


FIG. 7: (Color online) Fourier transform of a randomly-selected cluster amplitude  $s_i^a$  or  $s_{ij}^{ab}$  for  ${}^{16}\text{O}$ . Energies are measured relative to the ground-state energy.

while the TDCC method requires one computation of  $\overline{H}_1$  per time step. The real advantage of the time-dependent coupled-cluster method lies – of course – in the study of time-dependent Hamiltonians.

### B. Excitation energies of interacting Lipkin systems

Hoodbhoy and Negele studied the dynamics of two interacting, 14-particle Lipkin models [40] with the TDCC method [13]. In this Subsection, we compare our calculations to the earlier results.

The  $N$ -particle Lipkin model consists of two  $N$ -fold

TABLE I: Comparison of select excited-state energies obtained via time-dependent CCSD (TD-CCSD) and equation-of-motion CCSD (EOM-CCSD) for  ${}^4\text{He}$ . Energies are given in units of MeV.

	TD-CCSD	EOM-CCSD
$E_1$	3.04	3.02
$E_2$	29.45	29.47
$E_3$	35.52	35.53
$E_4$	41.10	41.11

TABLE II: Comparison of select excited-state energies obtained via time-dependent CCSD (TD-CCSD) and equation-of-motion CCSD (EOM-CCSD) for  ${}^{16}\text{O}$ . Energies are given in units of MeV.

	TD-CCSD	EOM-CCSD
$E_1$	32.20	32.29
$E_2$	33.85	33.91
$E_3$	37.40	37.60
$E_4$	48.15	48.12

degenerate levels separated by an energy  $\varepsilon$ . In the reference state, all  $N$  particles occupy the lower level. The particles interact via the two-body Hamiltonian

$$H = \frac{\varepsilon}{2} \sum_{p\sigma} \sigma a_{p\sigma}^\dagger a_{p\sigma} + \frac{V}{2} \sum_{pq\sigma} a_{p\sigma}^\dagger a_{q\sigma}^\dagger a_{q-\sigma} a_{p-\sigma}. \quad (46)$$

Here  $p, q = 1, \dots, N$  are particle labels,  $\sigma = \pm 1$  denotes the upper and lower level, respectively, and  $V$  is the strength of the two-body interaction. For weak interactions  $V(N-1) < \varepsilon$ , the reference state is  $\prod_{p=1}^N a_{p-}^\dagger |0\rangle$ , and the model is in its “symmetric” phase. At  $V(N-1) \approx \varepsilon$  the model makes a transition to a “deformed” phase, and a Hartree-Fock reference state should be chosen for  $V(N-1) > \varepsilon$ .

As in Ref. [13] we consider two Lipkin models ( $N = 14$  each with Hamiltonians  $H_1$  and  $H_2$ , respectively) that are noninteracting for  $t < 0$  and start to interact at  $t = 0$  via

$$H_{\text{int}} = V \sum_{p_1 p_2 \sigma} a_{p_1 \sigma}^\dagger a_{p_2 \sigma}^\dagger a_{p_2 - \sigma} a_{p_1 - \sigma}. \quad (47)$$

The observable of interest is the energy difference

$$\Delta E(t) \equiv \frac{1}{2} \left( \langle \Psi | H_1 + H_2 | \Psi \rangle(t) - \langle \Psi | H_1 + H_2 | \Psi \rangle(0) \right) \quad (48)$$

of the subsystems.

In Hoodbhoy and Negele’s calculation only  $2p$ - $2h$  excitations were considered (setting  $S_1 = 0$ ), and Eq. (14) is solved. The calculation of expectation values was performed in a Hermitian approach based on the density matrices

$$(\rho_{qp})_N = \langle \Phi | e^{S^\dagger} \{p^\dagger q\} e^S | \Phi \rangle_C, \quad (49)$$

$$(\rho_{rspq})_N = \langle \Phi | e^{S^\dagger} \{p^\dagger q^\dagger sr\} e^S | \Phi \rangle_C. \quad (50)$$

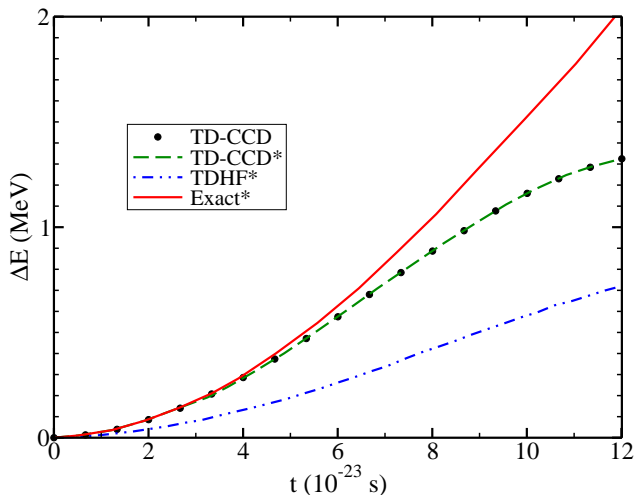


FIG. 8: (Color online) Time-dependent coupled-cluster doubles (TD-CCD) result for the excitation energy as a function of time for two interacting, 14-particle Lipkin systems. Hoodbhoy and Negele’s results for TD-CCD, time-dependent Hartree-Fock (TDHF), and the exact calculation are noted with an asterisk and were taken from Ref. [13].

Here the subscripts  $N$  and the curly brackets indicate the normal-ordering of the creation and annihilation operators. The subscript  $C$  indicates that the disconnected diagrams have been factored from the expressions. Whereas these expressions can easily be expanded in terms of products of the cluster amplitudes  $s_i^a$  and  $s_{ij}^{ab}$ , the expansions are non-terminating due to the exponential nature of the excitation operators. Thus they must be truncated at some level, and we choose a truncation at the terms quadratic in the  $s_{ij}^{ab}$  amplitudes. Setting  $\varepsilon = 1$  and  $V = 0.357$  for strong coupling, we computed the excitation energy of each system as a function of time for  $12 \times 10^{-23}$  s, making 90 time steps of size 0.4 fm/c. Our result for the excitation energy and that obtained by Hoodbhoy and Negele [13] are shown in Fig. 8. The results are indistinguishable. Figure 8 also shows the exact results and results from time-dependent Hartree-Fock (both taken from Ref. [13]).

Let us finally also compute time-dependent expectation values within the coupled-cluster framework and employ the evolution of the left de-excitation operator  $L$  and the density matrix (26) of the 14-particle Lipkin system. The parameters of the Lipkin model are  $\varepsilon = 1$  and  $V = 0.04$ . Thus,  $(N - 1)V \approx 0.52 < 1$ , and we are in the symmetric phase of the two-level Lipkin model. We choose the initial conditions  $S = 0 = L$  and study the time evolution of the operator

$$J_z = \frac{1}{2} \sum_{p\sigma} \sigma a_{p\sigma}^\dagger a_{p\sigma}. \quad (51)$$

Our result shown in Fig. 9 exhibits a good agreement with the exact solution. The main period and amplitude of

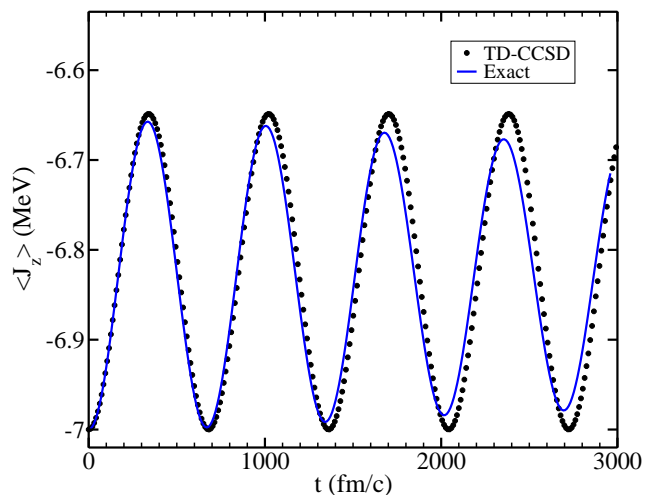


FIG. 9: (Color online) Time-dependent CCSD evolution of the one-body interaction of the 14-particle Lipkin system. The exact result is also shown.

the oscillation is well reproduced but the coupled-cluster calculation misses a fine modulation of the amplitude. We also performed computations for weaker interaction strengths  $V$  and observed that the agreement between TDCC theory and the exact solution improves with decreasing values of the interaction strength.

## V. CONCLUSIONS

We have studied the bi-variational formulation of time-dependent coupled-cluster theory and illustrated some of its features in applications to simple models of the atomic nuclei. Our main results are (i) the explicit demonstration that observables that commute with the Hamiltonian are conserved under time evolution, (ii) the explanation of the role of the similarity-transformed Hamiltonian under real and imaginary time evolution, and (iii) the computation of energy spectra and time-dependent observables and their comparison with exact results within simple models. These results open the way for the description of time-dependent phenomena such as nuclear collisions within more realistic models and beyond time-dependent mean-field methods.

## Acknowledgments

The authors thank G. F. Bertsch, D. J. Dean, S. Kvaal, and S. Umar for discussions. This work has been supported by the U.S. Department of Energy under grant Nos. DE-FG02-96ER40975 (Vanderbilt University) and DE-FG02-96ER40963 (University of Tennessee) and DE-AC05-00OR22725 with UT-Battelle, LLC (Oak Ridge National Laboratory). This research used resources of



the Oak Ridge Leadership Computing Facility at the Oak Ridge National Laboratory.

### Appendix A: Equations (12), (13), and (14) in a time-dependent basis

If the single-particle states are allowed to time-evolve, the commutator in Eq. (11) is nonzero, and the equations of motion for the cluster amplitudes become

$$\langle \Phi | \bar{H} | \Phi \rangle = i\hbar \left[ \dot{s}_0 + \sum_k \langle k | \dot{k} \rangle + \sum_{kc} s_k^c \langle k | \dot{c} \rangle \right], \quad (\text{A1})$$

$$\begin{aligned} \langle \Phi_i^a | \bar{H} | \Phi \rangle = i\hbar & \left[ \dot{s}_i^a + \langle a | \dot{i} \rangle \right. \\ & + \sum_c s_i^c \langle a | \dot{c} \rangle + \sum_k s_k^a \langle i | \dot{k} \rangle^* \\ & + \frac{1}{2} \sum_{kc} s_k^a s_i^c \left( \langle c | \dot{k} \rangle^* - \langle k | \dot{c} \rangle \right) \\ & \left. + \sum_{kc} s_{ki}^{ca} \left( \langle k | \dot{c} \rangle + \langle c | \dot{k} \rangle^* \right) \right], \quad (\text{A2}) \end{aligned}$$

$$\begin{aligned} \langle \Phi_{ij}^{ab} | \bar{H} | \Phi \rangle = i\hbar & \left[ \dot{s}_{ij}^{ab} + \sum_c (s_{ij}^{cb} \langle a | \dot{c} \rangle - s_{ij}^{ca} \langle b | \dot{c} \rangle) \right. \\ & + \sum_k (s_{kj}^{ab} \langle i | \dot{k} \rangle - s_{ki}^{ab} \langle j | \dot{k} \rangle) \\ & + \frac{1}{2} P(ab) \sum_{kc} s_k^a s_{ij}^{cb} \left( \langle c | \dot{k} \rangle^* - \langle k | \dot{c} \rangle \right) \\ & \left. + \frac{1}{2} P(ij) \sum_{kc} s_i^c s_{kj}^{ab} \left( \langle c | \dot{k} \rangle^* - \langle k | \dot{c} \rangle \right) \right]. \quad (\text{A3}) \end{aligned}$$

- 
- [1] F. Coester, Nucl. Phys. **7**, 421 (1958).
  - [2] F. Coester and H. Kümmel, Nucl. Phys. **17**, 477 (1960).
  - [3] J. Cizek, J. Chem. Phys. **45**, 4256 (1966).
  - [4] J. Cizek, Adv. Chem. Phys. **14**, 35 (1969).
  - [5] J. Paldus and X. Li, Adv. Chem. Phys. **110**, 1 (1999).
  - [6] R. F. Bishop, Theor. Chim. Acta **80**, 95 (1991).
  - [7] T. Crawford and H. Schaefer, Rev. Comp. Chem. **14**, 33 (2000).
  - [8] R. J. Bartlett and M. Musiał, Rev. Mod. Phys. **79**, 291 (2007).
  - [9] I. Shavitt and R. Bartlett, *Many-Body Methods in Chemistry and Physics: MBPT and Coupled-Cluster Theory* (Cambridge, 2009).
  - [10] P. Navrátil, S. Quaglioni, I. Stetcu, and B. R. Barrett, J. Phys. G **36**, 083101 (2009).
  - [11] G. Hagen, T. Papenbrock, D. J. Dean, and M. Hjorth-Jensen, Phys. Rev. Lett. **101**, 092502 (2008).
  - [12] G. Hagen, T. Papenbrock, D. J. Dean, and M. Hjorth-Jensen, Phys. Rev. C **82**, 034330 (2010).
  - [13] P. Hoodbhoy and J. W. Negele, Phys. Rev. C **18**, 2380 (1978).
  - [14] P. Hoodbhoy and J. W. Negele, Phys. Rev. C **19**, 1971 (1979).
  - [15] K. Schönhammer and O. Gunnarson, Phys. Rev. B **18**, 6606 (1978).
  - [16] P. A. M. Dirac, Proc. Cambridge Phil. Soc. **26**, 376 (1930).
  - [17] P. Bonche, S. Koonin, and J. W. Negele, Phys. Rev. C **13**, 1226 (1976).
  - [18] D. M. Brink, M. J. Giannoni, and M. Vénérioni, Nuc. Phys. A **258**, 237 (1976).
  - [19] A. S. Umar and V. E. Oberacker, Phys. Rev. C **76**, 014614 (2007).
  - [20] H.-D. Meyer, F. Gatti, and G. A. Worth, *Multidimensional Quantum Dynamics: MCTDH Theory and Applications* (Wiley, 2009).
  - [21] E. Dalggaard and H. J. Monkhorst, Phys. Rev. A **28**, 1217 (1983).
  - [22] H. Sekino and R. J. Bartlett, Int. J. Quan. Chem. **18**, 255 (1984).
  - [23] K. L. Sebastian, Phys. Rev. B **31**, 6976 (1985).
  - [24] H. J. Monkhorst, Phys. Rev. A **36**, 1544 (1987).
  - [25] H. Koch and J. Jørgensen, J. Chem. Phys. **93**, 3333 (1990).
  - [26] G. Sree Latha and M. Durga Prasad, J. Chem. Phys. **105**, 2972 (1996).
  - [27] M. Durga Prasad, Int. J. Mol. Sci. **3**, 447 (2002).
  - [28] C. Huber and T. Klamroth, J. Chem. Phys. **134**, 054113 (2011).
  - [29] M. Takahashi and J. Paldus, J. Chem. Phys. **85**, 1486 (1986).

- (1986).
- [30] S. Kvaal (2012), arXiv:1201.5548.
- [31] J. Arponen, Ann. Phys. **151**, 311 (1983).
- [32] J. Stanton and R. Bartlett, J. Chem. Phys. **98**, 7029 (1993).
- [33] S. K. Bogner, R. J. Furnstahl, and A. Schwenk, Prog. Part. Nucl. Phys. **65**, 94 (2010).
- [34] D. R. Entem and R. Machleidt, Phys. Rev. C **68**, 041001 (2003).
- [35] S. D. Glazek and K. G. Wilson, Phys. Rev. D **48**, 5863 (1993).
- [36] F. Wegner, Ann. Phys. (Leipzig) **506**, 77 (1994).
- [37] S. K. Bogner, R. J. Furnstahl, and R. J. Perry, Phys. Rev. C **75**, 061001 (2007).
- [38] K. Tsukiyama, S. K. Bogner, and A. Schwenk, Phys. Rev. Lett. **106**, 222502 (2011).
- [39] G. Hagen, T. Papenbrock, and D. J. Dean, Phys. Rev. Lett. **103**, 062503 (2009).
- [40] H. J. Lipkin, N. Meshkov, and A. J. Glick, Nucl. Phys. **62**, 188 (1965).